

# Structure and Function of Enzymes Adsorbed onto Single-Walled Carbon Nanotubes

Sandeep S. Karajanagi, Alexey A. Vertegel, Ravi S. Kane,\* and Jonathan S. Dordick\*

Department of Chemical and Biological Engineering, Rensselaer Polytechnic Institute, Troy, New York 12180

Received August 10, 2004. In Final Form: September 27, 2004

We have examined the structure and function of two enzymes,  $\alpha$ -chymotrypsin (CT) and soybean peroxidase (SBP), adsorbed onto single-walled carbon nanotubes (SWNTs). SBP retained up to 30% of its native activity upon adsorption, while the adsorbed CT retained only 1% of its native activity. Analysis of the secondary structure of the proteins via FT-IR spectroscopy revealed that both enzymes undergo structural changes upon adsorption, with substantial secondary structural perturbation observed for CT. Consistent with these results, AFM images of the adsorbed enzymes indicated that SBP retains its native three-dimensional shape while CT appears to unfold on the SWNT surface. This study represents the first in depth investigation of protein structure and function on carbon nanotubes, which is critical in designing optimal carbon nanotube–protein conjugates.

## Introduction

Single-walled carbon nanotubes (SWNTs) have rapidly become one of the most widely studied nanomaterials, primarily because of their unique physicochemical properties and wide-ranging applications in solid-state nanoelectronics, nanocomposites, nanolithography, sensing, and high-resolution imaging.<sup>1</sup> To realize these applications, various methods of functionalization are being developed to interface the SWNTs with organic and inorganic materials, as well as biological macromolecules. The latter is gaining popularity because of potential applications in biosensor development,<sup>2</sup> bioelectrochemistry,<sup>3</sup> biomedical devices,<sup>4</sup> and cellular delivery of peptides and proteins.<sup>5,6</sup> Covalent functionalization of SWNTs<sup>7</sup> with proteins has been demonstrated by reacting the free amine groups on the surface of a protein with carboxylic acid groups that were generated by sidewall oxidation of SWNTs and subsequently activated using carbodiimide. Though covalent immobilization of proteins onto SWNTs leads to stable protein attachment, the chemical modification of the SWNT surface may compromise the desirable electronic and mechanical properties of the SWNTs. Conversely, noncovalent functionalization of SWNTs<sup>2,8–11</sup> with proteins preserves the native structural and functional properties of the nanotubes.

Various methods of noncovalent attachment of proteins onto SWNTs have been explored. These include the direct

physical adsorption of proteins onto the hydrophobic surface,<sup>9</sup> immobilization using surfactants (e.g., Tween-20 and Triton X-100),<sup>2,10,11</sup> or functionalization using adsorbed polymer layers.<sup>2,8</sup> For example, coadsorption of Triton X-100<sup>10</sup> or Triton X-405 with poly(ethylene glycol) (PEG) onto SWNTs can be used for selective immobilization of proteins.<sup>11</sup> Alternatively, adsorption of poly(ethylene oxide) (PEO)-containing surfactants such as Tween 20 and Pluronic P103 onto the surface of SWNTs can then be followed by the covalent coupling of proteins (e.g., Streptavidin, Staphylococcal protein A, and U1A) to the PEO chains using 1,1-carbonyldiimidazole activation.<sup>2</sup> In all cases, the attachment process does not appear to alter the structure and material properties of the nanotubes.

Despite this growing interest in preparing protein–nanotube “hybrids”, relatively little is known about the structure, function, and spatial orientation of proteins noncovalently adsorbed onto carbon nanotubes. The catalytic activity and exquisite selectivity of proteins requires the near complete retention of native structure. It is therefore important to understand how the SWNT surface affects the structure and function of adsorbed proteins. For this reason, we embarked on a study to elucidate the structure and function of enzymes adsorbed directly onto SWNTs. Using enzymes as highly sensitive probes of protein function, we demonstrate that protein structure and function is strongly influenced by the hydrophobic, nanoscale environment of a SWNT. Moreover, depending on the nature of the protein, the SWNT can promote retention or loss of natelike protein properties. This study represents the first in depth evaluation of both the structure and function of proteins adsorbed onto carbon nanotubes. This information

\* Authors to whom correspondence should be addressed. E-mail: dordick@rpi.edu (J.S.D.); kaner@rpi.edu (R.S.K.).

(1) Ajayan, P. M. *Chem. Rev.* **1999**, *99*, 1787.  
 (2) Chen, R. J.; Bangsaruntip, S.; Drouvalakis, K. A.; Kam, N. W. S.; Shim, M.; Li, Y.; Kim, W.; Utz, P. J.; Dai, H. *Proc. Natl. Acad. Sci. U.S.A.* **2003**, *100*, 4984.  
 (3) Gooding, J. J.; Wibowo, R.; Liu, J.; Yang, W.; Losic, D.; Orbons, S.; Mearns, F. J.; Shapter, J. G.; Hibbert, D. B. *J. Am. Chem. Soc.* **2003**, *125*, 9006.  
 (4) Baughman, R. H.; Changxing, C.; Zakhidov, A. A.; Iqbal, Z.; Barisci, J. N.; Spinks, G. M.; Wallace, G. G.; Mazzoldi, A.; Rossi, D. D.; Rinzler, A. G.; Jaschinski, O.; Roth, S.; Kertesz, M. *Science* **1999**, *284*, 1340.  
 (5) Pantarotto, D.; Briand, J.-P.; Prato, M.; Bianco, A. *Chem. Commun.* **2004**, *1*, 16.  
 (6) Kam, N.; Jessop, T. C.; Wender, P. A.; Dai, H. *J. Am. Chem. Soc.* **2004**, *126*, 6850.  
 (7) Weijie, H.; Taylor, S.; Fu, K.; Lin, Y.; Zhang, D.; Hanks, T. W.; Rao, A. M.; Sun, Y.-P. *Nano Lett.* **2002**, *2*, 311.

(8) Carrillo, A.; Swartz, J. A.; Gamba, J. M.; Kane, R. S.; Chakrapani, N.; Wei, B.; Ajayan, P. M. *Nano Lett.* **2003**, *3*, 1437.

(9) Erlanger, B. F.; Chen, B.-X.; Zhu, M.; Brus, L. *Nano Lett.* **2001**, *1*, 465.

(10) Panhius, M.; Salvador-Morales, C.; Franklin, E.; Chambers, G.; Fonseca, A.; Nagy, J. N.; Blau, W. J.; Minett, A. I. *J. Nanosci. Nanotech.* **2003**, *3*, 209.

(11) Shim, M.; Kam, N. W. S.; Chen, R. J.; Li, Y.; Dai, H. *Nano Lett.* **2002**, *2*, 285.

is critical for the design of functional protein-containing nanocomposites.

### Experimental Section

**Materials.** Raw SWNTs were purchased from Carbon Nanotechnologies, Inc. (Houston, TX) and used without further purification. Soybean Peroxidase (SBP),  $\alpha$ -Chymotrypsin from bovine pancreas (CT), and *N*-succinyl-L-alanyl-L-alanyl-L-proline-L-phenyl-L-nitroanilide (tetrapeptide) were purchased from Sigma-Aldrich (St. Louis, MO) as salt-free, dry powders and used without further purification. Bichinchoninic Acid (BCA) assay reagents used for determining solution phase protein concentrations were purchased from Pierce Biotechnology, Inc. (Rockford, IL). All other chemicals were purchased from Sigma-Aldrich (St. Louis, MO) and used as obtained.

**Enzyme Adsorption onto SWNTs.** Enzymes were immobilized on SWNTs using physical adsorption. SWNTs were sonicated in dimethylformamide (DMF) for 30 min to obtain a uniform dispersion. SWNTs (1 mg) were then dispensed into an Eppendorf microcentrifuge tube, and the organic phase was gradually replaced by an aqueous phase through repeated washing with pH 7.0 buffer (50 mM phosphate). This gradual change from organic phase to an aqueous phase renders unfunctionalized SWNTs more dispersible in water. The dispersion of SWNTs in the aqueous buffer was then exposed to a freshly prepared solution of enzyme in the same buffer, and the mixture was shaken on an Innova 2000 (New Brunswick Scientific Co., Inc., Edison, NJ) platform shaker for 2 h at 200 rpm and room temperature. In the case of CT, the shaking was carried out at 4 °C to prevent autolysis during incubation. After incubation, the SWNTs were centrifuged at about 8000 rpm using a microcentrifuge and the supernatant was removed. Typically, six washes were performed, with fresh buffer added each time to remove unbound enzyme. All supernatants were analyzed for protein content using the BCA or the  $\mu$ BCA assay. The amount of enzyme loaded onto the SWNTs was determined by measuring the difference in the concentration of enzyme in solution before and after exposing it to the dispersion of SWNTs in buffer.

**Atomic Force Microscopy Experiments.** Atomic Force Microscopy (AFM) images for enzymes adsorbed onto SWNTs were obtained by using a Nanoscope III Multimode scanning probe microscope (Digital Instruments, Veeco Metrology Group, Santa Barbara, CA) in the tapping mode. Typically, enzymes were adsorbed onto SWNTs using the procedure outlined above. A dilute suspension of the SWNT-enzyme composite ( $\sim 30 \mu\text{g/mL}$ ) was then prepared in MilliQ water, and  $30 \mu\text{L}$  of the dispersion was placed onto a freshly cleaved mica surface. The sample was then air-dried and analyzed by AFM.

**Determination of Enzyme Activity.** The activity of SBP was measured using *p*-cresol as the substrate. SBP catalyzes the oxidation of *p*-cresol in the presence of  $\text{H}_2\text{O}_2$  to form fluorescent oligo- and polyphenol products. For a typical solution-phase assay,  $0.15 \mu\text{g/mL}$  SBP was used with 20 mM *p*-cresol and 0.125 mM  $\text{H}_2\text{O}_2$  in a volume of  $200 \mu\text{L}$ . All solutions were prepared in pH 7.0 buffer (50 mM phosphate) containing 20% (v/v) DMF. The initial reaction rates were then measured by tracking the increase in fluorescence of the reaction mixture at excitation and emission wavelengths of 325 and 402 nm, respectively, using an HTS 7000 Plus Bio Assay Reader (Perkin-Elmer, Wellesley, MA). To measure the activity of SBP adsorbed onto SWNTs (SWNT-SBP), a well-mixed dispersion of SWNT-SBP at a concentration of 1.0 mg/mL was prepared in aqueous buffer. A known amount of SWNT-SBP was then dispensed via serial dilution. For a typical experiment, 0.2–2.5  $\mu\text{g}$  of SWNTs were used on the basis of the loading of SBP. The enzymatic activity was measured as described above. A small fraction of the adsorbed enzyme leached during the serial dilutions. To account for this leached enzyme, we washed the SWNT-SBP suspension six times using the same dilutions and buffer as those used in the final activity measurement. Since the amount of leached enzyme during these washes was too low ( $< 15 \text{ ng/mL}$ ) to be reliably detected by protein assays, we estimated protein concentration in the washes via activity measurements and assumed that the activity of the leached enzyme was identical to that of native enzyme. Using the value of specific activity of the solution-phase enzyme and the initial

rate of reaction for the enzyme in the wash solution, the concentration of enzyme present in the washes was determined. The final loading of SBP on the SWNTs was then calculated. The total amount of enzyme leached during these washes was  $< 10\%$  of the loading on the SWNTs before the washes. After washing, the SWNT-SBP was dispersed into aqueous buffer and assayed as previously described. Periodically, the SWNTs were centrifuged at about 8000 rpm using a microcentrifuge and the fluorescence of a  $200 \mu\text{L}$  aliquot of the supernatant was measured. The aliquot was then replaced in the reaction mixture. Fluorescence was correlated to the concentration of  $\text{H}_2\text{O}_2$  consumed as described by Ryu and Dordick.<sup>12</sup>

The activity of CT was measured using tetrapeptide as the substrate. For a typical solution phase assay,  $1.25 \mu\text{g/mL}$  of freshly prepared CT was incubated with a  $100 \mu\text{M}$  solution of tetrapeptide in phosphate buffer (50 mM, pH 8.0). CT catalyzes the hydrolytic cleavage of the substrate that releases the chromophore, *p*-nitroaniline, which absorbs at 405 nm. The activity of the enzyme was obtained by measuring the increase in the absorbance of the reaction mixture at 405 nm and standardized via the experimentally determined extinction coefficient ( $\epsilon_{405} = 14,250 \text{ M}^{-1} \text{ cm}^{-1}$ ). The activity of CT adsorbed onto SWNTs (SWNT-CT) was measured using a technique identical to that used for adsorbed SBP (see above). For SWNT-CT, 4–50  $\mu\text{g}$  of functionalized SWNTs were used for the measurement of activity on the basis of the loading of CT. After performing six washes similar to those done for SWNT-SBP, the SWNT-CT was dispersed in aqueous buffer and assayed as described above. The dispersion was well mixed by shaking at 150 rpm at all times during the reaction using the platform shaker. Periodically, the SWNTs were centrifuged at about 8000 rpm using a microcentrifuge, and the absorbance of the supernatant was measured at 405 nm.

**FT-IR Spectroscopy.** The secondary structure of native and adsorbed enzymes was determined using FT-IR spectroscopy. All spectra were collected using a Nicolet Magna 550 series II FT-IR spectrometer with a horizontal ATR accessory obtained from SpectraTech, Inc. (Thermo Electron Corporation, Waltham, MA). The spectrometer was equipped with a mercury cadmium telluride detector cooled by liquid nitrogen. The IR system was continuously purged with dry air from a Balston Purge Gas Generator (Thermo Electron Corporation, Waltham, MA) to reduce the interference due to water vapor and carbon dioxide. The data collection and second-derivative calculations were carried out using the software OMNIC 6.1a provided by Thermo Nicolet Corporation.

All experiments involving solution-phase enzymes were carried out using attenuated total reflection (ATR) FT-IR spectroscopy using a Germanium crystal. An average of 512 scans were obtained at a resolution of  $2 \text{ cm}^{-1}$  with a gain of 2 and an aperture of 50. Enzyme solutions (25 mg/mL) in  $\text{D}_2\text{O}$  were used for the experiments. The spectrum of pure  $\text{D}_2\text{O}$  was subtracted from the spectra of the enzyme solutions to obtain the spectra of only the enzymes. The FT-IR spectra for enzymes adsorbed onto SWNTs were obtained using the spectrometer in the transmission mode between 4000 and  $500 \text{ cm}^{-1}$ . Typically, 1 mg of SWNT-enzyme composite was prepared as described above. The unbound enzyme was washed extensively with MilliQ water. The sample was then lyophilized (LabConco, Kansas City, MO). Lyophilized SWNT-enzyme composite (1 mg) was then ground with about 40–50 mg of IR grade KBr to form a homogeneous powder. The grinding was performed under a nitrogen atmosphere to prevent absorption of atmospheric water during the grinding procedure. About 30 mg of the powder was then used to form a pellet that was used to obtain an FT-IR absorbance spectrum. This method does not introduce artificial structural changes in the protein.<sup>13</sup> The pellet was then vacuum-dried to remove atmospheric water. The vacuum-dried pellet was immediately transferred into the FT-IR chamber using a desiccator to transport the pellet. The sample compartment was purged with dry air for 1 h before collecting the FT-IR spectra of the adsorbed enzymes. All scans reported were an average of 1024 scans obtained at a resolution of  $4 \text{ cm}^{-1}$  with a gain of 1 and an aperture of 50. The FT-IR spectrum of

(12) Ryu, K.; Dordick, J. S. *Biochemistry* **1992**, *31*, 2588.

(13) Meyer, J. D.; Manning, M. C.; Carpenter, J. F. *J. Pharm. Sci.* **2004**, *93*, 496.

the unfunctionalized SWNTs (control sample) was obtained in an identical manner. Care was taken to ensure that the control sample used for obtaining the FT-IR spectrum had an identical amount of SWNTs to that used for the SWNT-enzyme sample. The spectrum of unfunctionalized SWNTs was subtracted from that of the SWNT-enzyme composite to obtain the spectrum of the adsorbed enzyme.

The spectra of the enzymes, both native and adsorbed, obtained after subtraction from the respective controls, were baseline corrected in the entire region. Corrections were made to the spectra to remove the effects due to water vapor and carbon dioxide in the optical path.

**Determination of Enzyme Secondary Structure.** Secondary structural contents of the enzymes were obtained by analyzing their FT-IR spectra in the amide I region from 1600 to 1700  $\text{cm}^{-1}$ . To obtain the second-derivative spectrum, the corrected spectra were smoothed once using a nine-point smoothing function.<sup>14</sup> Care was taken to obtain a straight baseline in the region from 1750 to 2000  $\text{cm}^{-1}$ , which is critical to obtain quantitative structural information using the second-derivative analysis method. Second derivatives of the baseline-corrected spectrum were obtained using a standard function in the commercial software. The second-derivative spectrum was then corrected in the region 1600–1700  $\text{cm}^{-1}$  to obtain a flat baseline. This spectrum was used to obtain the  $\alpha$ -helix and  $\beta$ -sheet contents of the enzymes.<sup>14</sup> The assignment of peaks to various secondary structural elements was performed as described in the literature.<sup>14–16</sup>

## Results and Discussion

Two structurally and functionally distinct enzymes,<sup>17</sup> CT and SBP, were adsorbed onto commercial SWNTs. The adsorption of SBP followed a pseudo-saturation behavior (Figure 1A), with a maximum loading of 575  $\mu\text{g}$  SBP/mg SWNTs. Adsorbed SBP had strong affinity for the SWNTs, with almost complete adsorption observed within the first minute. Protein adsorption was irreversible at lower loadings. For example, at a loading of 250  $\mu\text{g}$  protein/mg SWNT, essentially no protein desorption was observed (Figure 1B). This result was not surprising given the propensity for proteins to adsorb irreversibly to hydrophobic surfaces<sup>18–20</sup> and is consistent with previous reports of protein adsorption onto SWNTs.<sup>21,22</sup> Similar behavior was seen for CT adsorbed onto SWNTs (data not shown) with a maximum loading of 673  $\mu\text{g}$  CT/mg SWNTs.

Although the adsorption behavior of the two enzymes was similar, the observed catalytic activities were vastly different. The specific activity of CT was no greater than 1% of native solution activity at all loadings tested (Figure 2). Conversely, SBP retained significant specific activity at all loadings (Figure 2) ranging from 18 to 280  $\mu\text{g}$  SBP/mg SWNTs (representing 3–50% of maximal surface coverage). The specific activity of SBP was strongly dependent on the loading; up to 28% of native solution activity was obtained at 50% of maximal surface coverage,

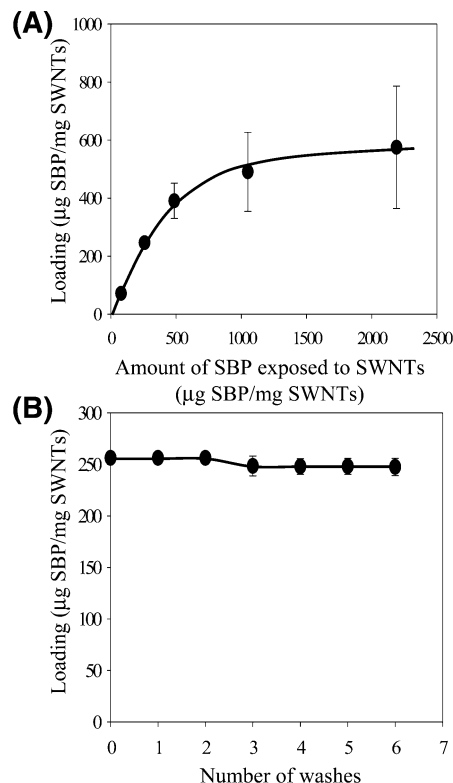


**Figure 1.** Loading of SBP on SWNTs: (A) Enzyme loading as a function of amount of SBP exposed to SWNTs. (B) Enzyme loading as a function of washing with fresh buffer. Each point represents an average of a minimum of three separate experiments, with some points showing error smaller than the symbol.

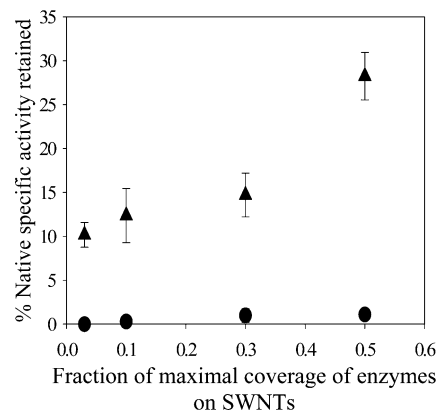


**Figure 2.** Enzymatic activity retained as a function of the surface coverage of the enzymes on SWNTs: adsorbed SBP ( $\blacktriangle$ ), adsorbed CT ( $\bullet$ ). Each point represents an average of a minimum of three separate experiments, with some points showing error smaller than the symbol. Specific activities above half-maximal coverage could not be obtained because of leaching of the adsorbed enzyme during activity measurement.

and this value dropped to ca. 10% at 3% of maximal surface coverage. The increase in specific activity of adsorbed SBP with an increase in the surface coverage on SWNTs may be due to the higher retention of native structure at higher surface loadings. This result is consistent with similar results obtained for other enzymes adsorbed on a range of surfaces and may be a result of increased crowding of the protein on the surface, thereby preventing inactivation due to surface spreading.<sup>23,24</sup>

(14) Dong, A.; Huang, P.; Caughey, W. S. *Biochemistry* **1990**, *29*, 3303.

(15) Griebenow, K.; Klivanov, A. M. *Biotechnol. Bioeng.* **1997**, *53*, 351.

(16) Vedantham, G.; Sparks, G. H.; Sane, S. U.; Tzannis, S.; Przybycien, T. *Anal. Biochem.* **2000**, *285*, 33.

(17) On the basis of the respective X-ray structures, CT is primarily a  $\beta$ -sheet protein,<sup>26</sup> while SBP is an  $\alpha$ -helix protein.<sup>28</sup> CT is a nonglycosylated serine protease with a pI of 8.1 while SBP is an oxidoreductase with a pI of 4.1 and is ca. 18% (w/w) glycosylated. The two model enzymes are thus structurally and functionally different.

(18) Norde, W. In *Surfactant Science Series*, 2nd ed.; Malmsten, M., Ed.; Marcel Dekker: New York, 2003; Vol. 110, p 21.

(19) Haynes, C. A.; Norde, W. *Colloids Surf., B* **1994**, *2*, 517.

(20) Arai, T.; Norde, W. *Colloids Surf.* **1990**, *51*, 1.

(21) Azamian, B. R.; Davis, J. J.; Coleman, K. S.; Bagshaw, C. B.; Green, M. L. H. *J. Am. Chem. Soc.* **2002**, *124*, 12664.

(22) Lin, Y.; Allard, L. F.; Sun, Y.-P. *J. Phys. Chem. B* **2004**, *108*, 3760.

(23) Zougrana, T.; Findenegg, G. H.; Norde, W. *J. Colloid Interface Sci.* **1997**, *190*, 437.

(24) Kondo, A.; Urabe, T. *J. Colloid Interface Sci.* **1995**, *174*, 191.



**Table 1. Secondary Structure of SBP and CT (Solution-Phase and Adsorbed onto SWNTs) as Determined by FT-IR Spectroscopy<sup>a</sup>**

sample	% $\alpha$ -helix	% $\beta$ -sheet
solution SBP	36.1 $\pm$ 1.2	25.1 $\pm$ 2.5
SBP adsorbed onto SWNTs	27.9 $\pm$ 4.1	20.6 $\pm$ 6.9
solution CT	13.6 $\pm$ 3.5	50.0 $\pm$ 2.4
CT adsorbed onto SWNTs	31.5 $\pm$ 2.9	23.5 $\pm$ 5.1

<sup>a</sup> The solution-phase secondary structure for CT matches well with the values obtained from the crystal structure. For SBP, however, the solution-phase  $\beta$ -sheet content does not correlate perfectly with that of the crystal structure. This may be because the crystal structure reported is for a nonglycosylated form of SBP,<sup>28</sup> while the native SBP used for this study is ca. 18% (w/w) glycosylated. It is known that glycosylation can change the secondary structure of a protein.<sup>29</sup> Nevertheless, a comparison can be made between different samples analyzed by the same method.

The observed disparity in catalytic activity between the two enzymes was intriguing and suggested that the SWNT surface affects the structures of the two enzymes in a fundamentally different manner. This prompted us to investigate the influence of the nanoscale environment on the structures of the two enzymes. To that end, transmission mode FT-IR spectroscopy was used to obtain the secondary structure of the adsorbed enzymes.<sup>25</sup> The relative amounts of SWNT–enzyme composite and KBr were carefully controlled to ensure a high signal-to-noise ratio. The FT-IR spectra were analyzed in the amide I region from 1600 to 1700  $\text{cm}^{-1}$ . This region, which consists mainly of the C=O stretching vibration of the backbone peptide bonds in proteins, has been used to estimate quantitatively the secondary structural features of proteins.<sup>26,27</sup> Table 1 provides a comparison of the secondary structural features calculated from the amide I spectra using the second-derivative method<sup>26</sup> for both enzymes in aqueous solution and enzymes adsorbed onto SWNTs (see Supporting Information for the assignments of peaks to secondary structural elements). The differences in secondary structure between the soluble and adsorbed states, as represented by the simple sum of magnitudes of changes in  $\alpha$ -helix and  $\beta$ -sheet contents, were ca. 13% and 44% for SBP and CT, respectively. Thus, both enzymes undergo a change in secondary structure upon adsorption; however, the change for CT is far more significant than that for SBP. Specifically, CT undergoes a substantial increase in  $\alpha$ -helix content concomitant with a dramatic decrease in its  $\beta$ -sheet content. A similar increase in  $\alpha$ -helix content was observed previously for CT adsorbed onto hydrophobic Teflon supports.<sup>23</sup> This significant change in the secondary structure of CT is consistent with its loss of activity on adsorption onto SWNTs.

Additional evidence of substantial structural perturbation of CT was obtained by using atomic force microscopy (AFM), which allowed us to obtain the “coarse-grained” three-dimensional structure of both enzymes on the SWNT surface. Such an approach, while not providing true tertiary structural information, nevertheless provides a quantitative measurement of the overall three-dimensional shape of the enzymes. Figure 3 shows AFM images of SBP adsorbed onto SWNTs at ca. half-maximal coverage. The wire-like structures represent bundles of 3–4

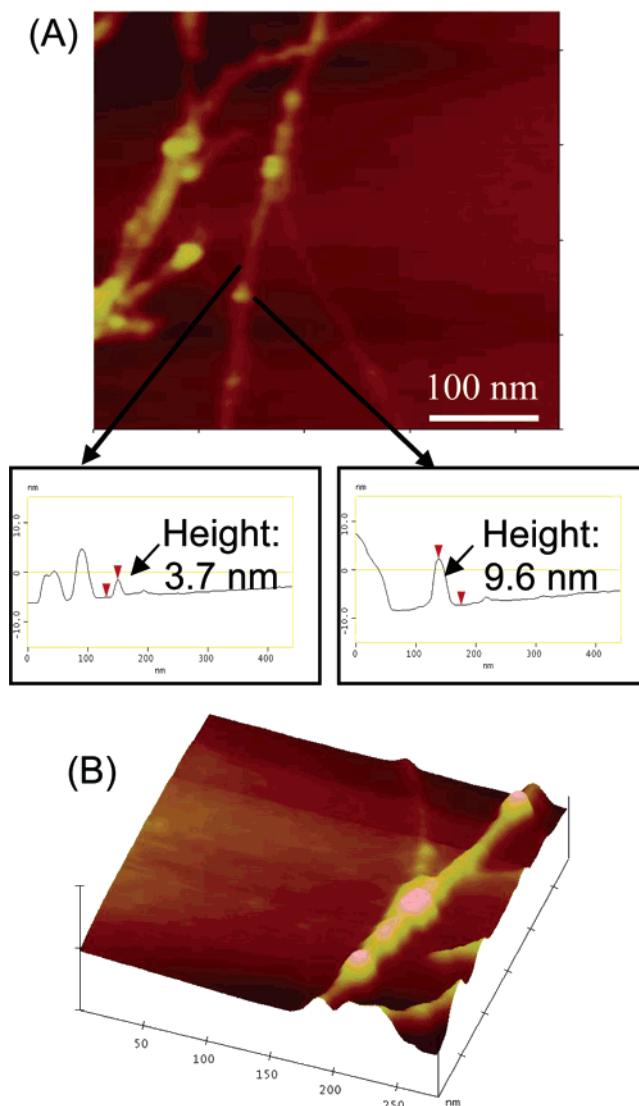


**Figure 3.** AFM images of SBP adsorbed onto SWNTs (half-maximal coverage): (A) The globular structures seen on the wirelike SWNTs represent SBP molecules. Line scans shown in the boxes reveal that a region on the SWNTs that does not contain SBP has a height of 3.7 nm, while a region containing SBP has a height of 9.6 nm, the difference (5.9 nm) being the height of adsorbed SBP molecules. (B) Surface plot of height image for SBP adsorbed onto SWNTs revealing SBP molecules on the SWNTs.

SWNTs, and the distinct globular structures on the SWNTs represent SBP molecules. Line scans revealed that the height of the globular structures ranged from 4 to 6 nm, which closely matches the molecular dimensions of SBP ( $6.1 \times 3.5 \times 4.0 \text{ nm}^3$ ).<sup>28</sup> The surface plot of SBP on SWNTs clearly reveals SBP molecules bound to a SWNT bundle (Figure 3B). These results suggest that SBP retains its native three-dimensional shape on the nanotube surface. The AFM of adsorbed CT, however, gave a vastly different image, where distinct enzyme molecules were not seen; rather, a layer of CT was observed (Figure 4). The height of the CT layer on the surface varied significantly, with values ranging from ca. 2 to 20 nm which are far different from the molecular size of CT ( $5.1 \times 4.0 \times 4.0 \text{ nm}^3$ ).<sup>23</sup> This result can be clearly seen in the surface plot of CT on SWNTs (Figure 4B). The presence of such a wide range of dimensions, and in particular, a

(25) Circular Dichroism spectroscopy could not be used for secondary-structure evaluation of the adsorbed enzyme because of interference due to SWNTs. Moreover, FT-IR spectroscopy in the ATR mode could not be used because of the tendency of the SWNTs to adsorb irreversibly to the Germanium crystal.

(26) Dong, A.; Huang, P.; Caghey, W. S. *Biochemistry* **1990**, *29*, 3303.

(27) Vedantham, G.; Sparks, H. G.; Sane, S. U.; Tzannis, S.; Przybycien, T. M. *Anal. Biochem.* **2000**, *285*, 33.

(28) Henriksen, A.; Mirza, O.; Indiani, C.; Teilum, K.; Smulevich, G.; Welinder, K. G.; Gajhede, M. *Protein Sci.* **2001**, *10*, 108.

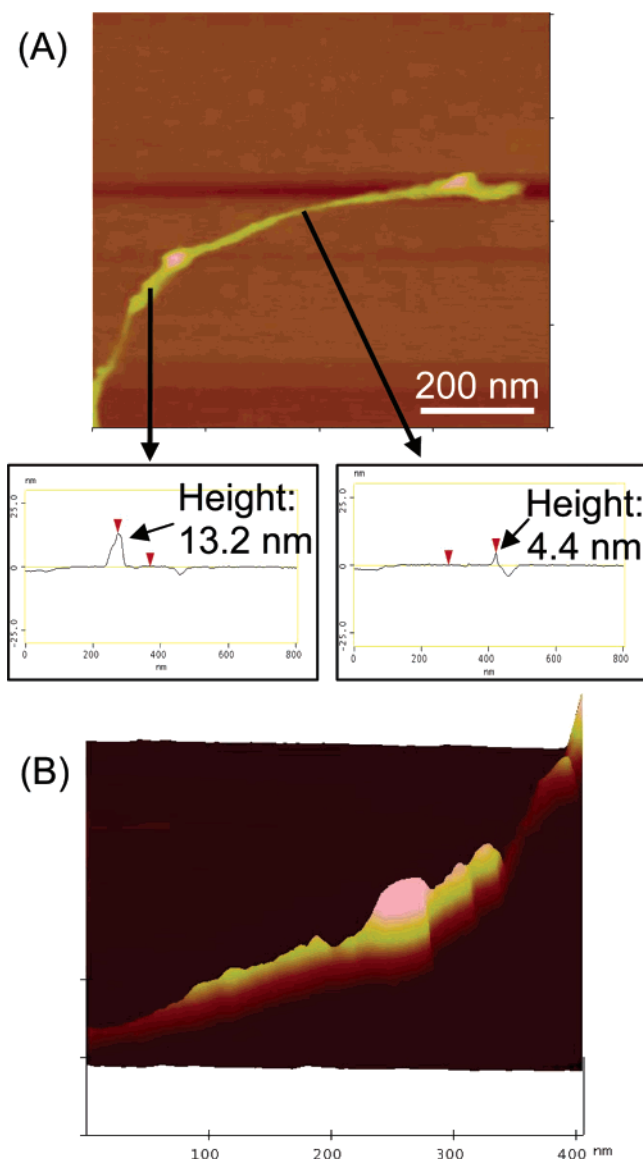


**Figure 4.** AFM images of CT adsorbed onto SWNTs (half monolayer coverage): (A) CT is seen to form a layer with varying heights on the SWNTs. Line scans shown in the boxes reveal that a region on the SWNTs that does not contain CT has a height of 4.4 nm, while a region containing CT has a height of 13.2 nm, the difference (8.8 nm) being the height of the CT layer. (B) Surface plot of height image for CT adsorbed onto SWNTs revealing a layer of CT on the SWNTs.

dimension as low as 2 nm, may indicate significant unfolding of CT upon adsorption onto SWNTs, resulting in a layer of enzyme spread across the hydrophobic surface. Such an event is likely to result in a higher propensity for protein aggregation, and this was observed with multiple protein layers with a thickness of up to 20 nm. This aggregation was not observed with SBP, and together with both the FT-IR and kinetic studies, these results indicate that CT undergoes substantial denaturation on the SWNT surface leading to its deactivation. SBP, in contrast, retains most of its native three-dimensional shape and has a smaller change in secondary structure, resulting in a greater retention of activity upon adsorption onto the SWNTs.

It is interesting that two enzymes, both monomeric and highly soluble in aqueous solutions, exhibited such drastically different behavior upon adsorption onto SWNTs. Although this phenomenon is not yet completely understood, one may speculate that SBP has evolved to

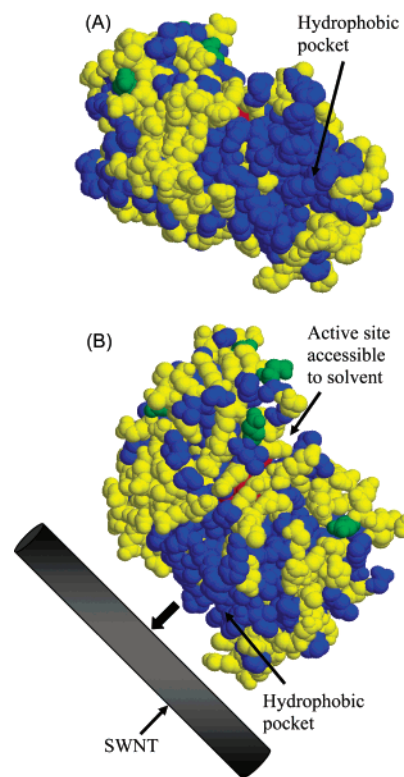


**Figure 5.** (A) PDB structure of SBP showing the hydrophobic pocket. Hydrophobic and hydrophilic residues are shown in blue and yellow, respectively, while the asparagine residues that are glycosylated are shown in green and the heme is shown in red. (B) A schematic hypothesizing the adsorption of SBP onto SWNTs via the hydrophobic pocket on SBP.

function in naturally hydrophobic environments to generate lignins and other polyphenols in plants.<sup>28</sup> SBP also has a high melting temperature,  $T_m$ , of ca. 90 °C,<sup>30</sup> while the  $T_m$  for CT is only 44 °C.<sup>31</sup> The greater stability of SBP in solution compared to that of CT may result in a higher structural integrity under denaturing conditions, such as the hydrophobic surface of a SWNT. A similar result was seen for lysozyme mutants adsorbed onto silica nanoparticles where a mutant with higher structural stability in solution retained more of its native structure upon adsorption.<sup>32</sup> The crystal structure of SBP<sup>28</sup> also reveals the presence of a cluster of 19 hydrophobic residues on the surface of SBP that constitute a hydrophobic pocket (Figure 5A). While SBP is glycosylated at asparagine residues 56, 130, 144, 185, 197, 211,<sup>34</sup> and possibly 216,<sup>35</sup> most of the glycosylation sites are distant from the hydrophobic pocket. It is therefore possible that the hydrophobic pocket on the SBP molecule preferentially interacts with the SWNTs, thereby orienting SBP in a specific conformation, without appreciable unfolding of the protein. A simple schematic of SBP adsorbed onto SWNTs via the hydrophobic pocket (Figure 5B) reveals that, in this particular orientation, the active site of SBP

(29) Huang, X.; Barchi, J. J., Jr.; Lung, F.-D. T.; Roller, P. P.; Nara, P. L.; Muschik, J.; Garrity, R. R. *Biochemistry* **1997**, *36*, 10846.

(30) McEldoon, J. P.; Dordick, J. S. *Biotechnol. Prog.* **1996**, *12*, 555.

(31) Carrasquillo, K. G.; Sanchez, C.; Griebenow, K. *Biotechnol. Appl. Biochem.* **2000**, *31*, 41.

(32) Billsten, P.; Wahlgren, M.; Arnebrant, T.; McGuire, J.; Elwing, H. *J. Colloid Interface Sci.* **1995**, *175*, 77.

(33) Frigerio, F.; Coda, A.; Pugliese, L.; Lionetti, C.; Menegatti, C.; Amiconi, G.; Schnebli, H. P.; Ascenzi, P.; Bolognesi, M. *J. Mol. Biol.* **1992**, *225*, 107.

(34) Welinder, K. G.; Larsen, Y. B. *Biochim. Biophys. Acta* **2004**, *1698*, 121.

(35) Gray, J. S. S.; Montgomery, R. *Glycobiology* **1997**, *7*, 679.

(containing a heme shown in red in the figure) is exposed to the solvent and is accessible to the substrate. A similar analysis of the crystal structure of CT,<sup>33</sup> however, does not reveal any large hydrophobic pocket, suggesting that CT must at least partially unfold in order to interact with the SWNT surface. This difference in the surface properties of SBP and CT might provide another explanation for the different extents of protein unfolding on the surface of SWNTs.

### Conclusions

In conclusion, we have demonstrated that different proteins interact differently with SWNTs. In what we believe is the first report on secondary structure and activity of enzymes adsorbed onto SWNTs, FT-IR spectroscopy provided clear evidence of secondary structural perturbations as a result of the protein interaction with the nanotube surface. The substantial structural perturbation for CT is consistent with its nearly complete loss in catalytic activity. SBP, however, clearly retains its native shape and a large fraction of its native secondary structure and is highly active on the hydrophobic nano-

material. Although it is unclear why the two enzymes behave so differently on the surface of the SWNTs, this study highlights the complexity of protein–material interactions at the nanoscale. Investigating the structure and function of proteins immobilized onto SWNTs, as shown in this study, will be critical for developing a better understanding of how proteins interact with SWNTs and eventually for the design of functional carbon nanotube–protein systems. This work is currently underway in our laboratories.

**Acknowledgment.** We acknowledge support from the NSF-Nanoscale Science and Engineering Center (DMR-0117792).

**Supporting Information Available:** Mean peak positions and assignments of secondary structural elements for solution phase and adsorbed enzymes, raw FT-IR spectra for unfunctionalized SWNTs and CT adsorbed onto SWNTs, and FT-IR spectra for solution-phase enzymes and adsorbed enzymes. This material is available free of charge via the Internet at <http://pubs.acs.org>.

LA047994H